Synthesis and vibrational analysis of N-(2′-Furyl)-Imidazole

ARTICLE *in* JOURNAL OF RAMAN SPECTROSCOPY · AUGUST 2009

Impact Factor: 2.67 · DOI: 10.1002/jrs.2219

Research Article

Journal of RAMAN SPECTROSCOPY

Received: 21 October 2008 Accepted: 31 December 2008 Published online in Wiley Interscience: 20 February 2009

(www.interscience.wiley.com) DOI 10.1002/jrs.2219

Synthesis and vibrational analysis of N-(2′-Furyl)-Imidazole

A. E. Ledesma,[a] J. Zinczuk,[b] A. Ben Altabef,[a] J. J. López González[c] and S. A. Brandán[a]*

The N-(2′-furyl)-imidazole (1) has been prepared and characterized using infrared, Raman and multidimensional nuclear magnetic resonance spectroscopies. Theoretical calculations have been carried out by employing the Density Functional Theory (DFT) method, in order to optimize the geometry of their two conformers in the gas phase and to support the assignments of the vibrational bands of 1 to their normal modes. For a complete assignment of the compound, DFT calculations were combined with Scaled Quamtum Mecanic Force Field (SQMFF) methodology in order to fit the theoretical wavenumber values to the experimental one. Furthermore, Natural Bond Orbital (NBO) and topological properties by Atoms In Molecules (AIM) calculations were performed to analyze the nature and magnitude of the intramolecular interactions. The result reveals that two conformers are expected in liquid phase.

Supporting information may be found in the online version of this article.

Keywords: N-(2′-furyl)-imidazole; synthesis; vibrational spectra; DFT calculations

Introduction

The furylimidazole compounds are aromatic heterocyclic compounds of great chemical interest because they are found as structural units of numerous types of drugs and polymers which are very important in biochemistry and pharmacology.[1–8] Compounds of this type interact with the recently discovered imidazoline receptors to give products of clinical use for hypertension, modulation of pituitary hormone release, depression, obesity, impotence, noninsulin-dependent diabetes and Alzheimer's disease.[6–8] All these important properties account for the interest in new and better strategies for the synthesis reactions in organic chemistry.[9–11] In previous papers we reported on the 2-(2′-furyl)-1*H*-imidazole and 2-(2′-furyl)-4,5-1*H*-dihydroimidazole compounds that were prepared and characterized by using infrared, Raman and multidimensional nuclear magnetic resonance spectroscopies.[12,13] In both molecules, two conformations of each species obtained by rotation of 180°, approximately, around the C–C inter-ring bond were detected. The crystal and molecular structure of both molecules were analysed by X-ray diffraction methods. In the first compound,[12] this method evidenced that both conformations are present in the lattice with equal occupancy and linked in an alternate way to the N–H–N bonded polymeric chains along the crystal [101] direction, while in the 2-(2′-furyl)-4,5-1*H*-dihydroimidazole compound, the X-ray diffraction results indicate that the anticonformer is the only present one in the crystalline state. In this latter compound, the molecules are arranged in the lattice as a polymeric structure that extends along the crystal a-axis. Complete assignments of the compounds were presented combining the Density Functional Theory calculations with the Pulay's SQMFF methodology in order to fit the theoretical wavenumber values to the experimental one. The N-Aryl imidazoles compounds are found in many biologically active compounds.[14] Nowadays, the Cu-based catalysts are the most effective systems for the N-Arylation of imidazoles.[15] Recently, Altman *et al*.[16] have reported for N-arylated compounds the synthesis methods by coupling imidazoles and benzimidazoles with aryl halides. We report here, the synthesis and the theoretical and experimental vibrational studies of N-(2′-furyl)-imidazole compound in order to effect a complete assignment of the vibrational spectra. Theoretical calculations have been carried out by employing the B3LYP method, in order to optimize the geometry in the gas phase and to confirm the assignments of the vibrational bands of N-(2′-furyl)-imidazole compound to their normal modes. The Natural Bond Orbital (NBO)[17–19] and topological properties by Atoms In Molecules (AIM)[20,21] calculations were also performed to analyze the energies and geometric parameters in the gas phase as well as the nature and magnitude of the intramolecular interactions. In addition, the observed multidimensional Nuclear Magnetic Resonance (NMR) spectrum for the compound is successfully compared with the chemical shift predicted by calculation for two conformers. In order to investigate the stability of the most stable conformer, additional calculations of the electrostatic potential (ESP)[22,23] derived from atomic charges were performed for both conformers.

* *Correspondence to: S. A. Brandán, Inquinoa-Conicet, Instituto de Química Física, Facultad de Bioquímica, Química y Farmacia, Universidad Nacional de Tucumán, San Lorenzo 456, T 4000 CAN,San Miguel de Tucumán, Tucumán, R. Argentina. E-mail: sbrandan@fbqf.unt.edu.ar*

a *Inquinoa-Conicet, Instituto de Química Física, Facultad de Bioquímica, Química y Farmacia, Universidad Nacional de Tucumán, San Lorenzo 456, T 4000 CAN,San Miguel de Tucumán, Tucumán, R. Argentina*

b *Instituto de Química Rosario (CONICET-UNR), Facultad de Ciencias Bioquímicas y Farmacéuticas, Suipacha 531, 2000 Rosario, Santa Fé, R. Argentina*

c *Departamento de Química Física y Analítica, Facultad de Ciencias Experimentales, Universidad de Jaén, 23071 Jaén, España*

Journal of RAMAN SPECTROSCOPY

Experimental

The compound was synthesized following the procedure used for the synthesis of N-(3′-furyl)-imidazole.[16] Using the catalyst system based in 4,7-dimethoxy-1,10-phenanthroline[16] in combination with Cu(I), Cs_2CO_3, DMSO as solvent and polyethyleneglycol (PEG) as additive, causes an increase in the yield of the desired product, decreasing the quantity of the dehalogenated furane byproduct.

An oven-dried screw-capped test tube was charged with a magnetic stir bar, Cu_2O (40 mg, 0.28 mmol), 4,7-dimethoxy-1,10-phenanthroline (180 mg, 0.75 mmol), imidazole (34 mg, 0.5 mmol), PEG (1 g), Cs_2CO_3 (2.28 g, 7 mmol). The reaction vessel was tight with a rubber plug, evacuated and back-filled with argon, and this sequence was repeated for an additional period. 2-Br-furane (0.53 ml, 6 mmol) and DMSO (2.5 ml) were then added successively. The sealed reaction tube was heated and stirred for 24 h in an oil bath at 110 °C. The reaction mixture was cooled at room temperature, diluted with dichloromethane (65 ml) and filtered through a plug of celite, eluting with additional dichloromethane. The filtrate was concentrated and the residue purified by flash chromatography on silica gel by using a mixture of hexane and ethyl acetate to give 318 mg of pure N-(2′-furyl) Imidazole as a pale yellow liquid. Yield: 47%.

The infrared spectrum of the compound was recorded between KBr windows from 4000 to 400 cm^{-1} on a FTIR GX1 spectrophotometer with a resolution of 1 cm^{-1} and 64 scans. The Raman spectrum was measured on the substance contained in a glass capillary with a Bruker IFS 66 with FRA 106 accessory with a resolution of 1 cm^{-1} and 100 scans (excitation line of 1064 nm, 800 mW of laser power). NMR spectra were recorded in CCl_3D diluted solutions using a Bruker 400 FT spectrometer at 400 and 25 MHz. All spectra were measured at room temperature.

^{1}HNMR (400 MHz, CCl_3D, 25 °C): δ = 6.14 (H14), 6.44 (H15), 7.13 (H8), 7.22 (H9), 7.26 (H16), 7.81 (H7) ppm.

^{13}CNMR (25 MHz, CCl_3D, 25 °C): δ = 144.49 (C6), 138.90 (C2), 135.43 (C12), 130.03 (C4), 117.60 (C5), 111.59 (C11), 96.25 (C10) ppm.

Mass spectrum *m/e* (relative intensity, %): 52 (40.2), 79 (20.7), 105 (14.4), 107 (30.4), 134 (M^+, 100).

Computational Details

The potential energy curve associated with the rotation around the O13-C6-N1-C2 dihedral angle for the molecule has been investigated by using the DFT method with the hybrid correlation functional B3LYP[24,25], B3P86[26] and B3PW91[27] with 6-31G* basis set. In all cases, the compound presents two stable structures of C_1 symmetries as can be seen in Fig. 1. The optimized geometries for the two conformations of **1** obtained in the potential energy curve, were obtained by using the B3LYP/6-31G* and B3LYP/6-311++G** methods. Furthermore, NBO calculations for the two conformations of **1** were performed at B3LYP/6-311++G** level using the NBO 3.1 program.[28] Atomic partial charges were calculated for both conformers from the ESP according to the Merz-Singh-Kollman scheme[29] at the same level theory, too. All calculations were performed by using the GAUSSIAN 03 program.[30]

The force field in Cartesian coordinates calculated at B3LYP/6-311++G** level for the two stable conformations of **1** were useful to get their corresponding harmonic vibrational wavenumbers. The resulting force fields were transformed to 'natural' internal coordinates with the MOLVIB program.[31,32] The natural coordinates are shown in Table S1 (Supporting Information), which were defined as proposed by Pulay *et al.*[33] with the labelling of the atoms corresponding to Fig. 1. In order to visualize the nature of the different molecular vibrations of both conformers of **1**, the Gauss View program for molecular graphical representations was used.[34] Following the SQMFF procedure[35–37], the harmonic force field for two conformers of this compound evaluated at B3LYP/6-311++G** level were scaled by transferring the recommended scaled factors of Rauhut and Pulay.[36,37] The potential energy distribution components (PED), larger than or equal to 10%, are subsequently calculated with the resulting Scaled Quantum Mechanics (SQM) force field.

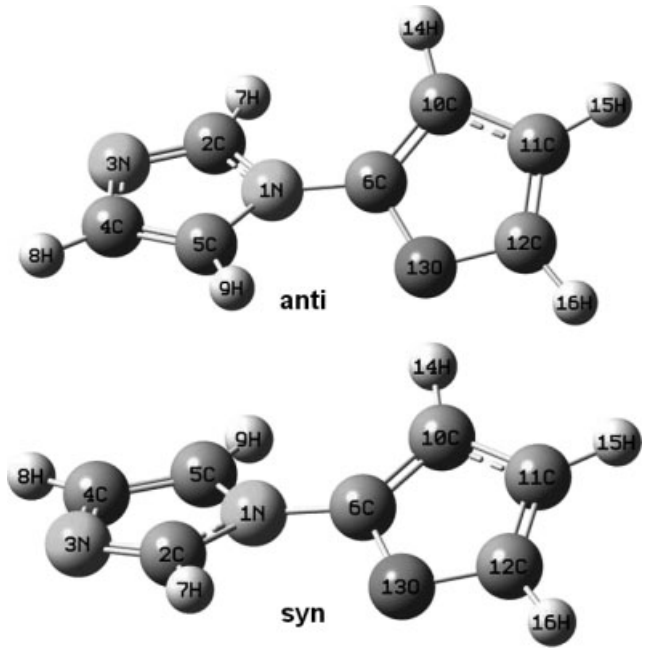

Figure 1. Theoretical structures and atoms numbering for *anti* and *syn* conformers of N-(2′-furyl)-imidazole.

Spectral analysis

Fourier self-deconvolution (FSD) is one of the most useful techniques to resolve overlapped bands into their components. It is based on the method described by Kauppinen *et al.*[38–40], where, defining only two enhancement factors W (bandwidth at half-height) and K (ratio of bandwidth of the enhanced and original bands), better resolved bands were obtained. This procedure was applied to the analysis of the infrared spectra by using Gaussian peak shapes and was performed using standard software.

In order to evaluate the presence of the two conformers in solution, the calculated chemical shifts of the ^{1}H NMR and ^{13}C NMR for both conformers were obtained by the GIAO method[41] by using the B3LYP/6-311++G** level of theory, as in similar molecules previously studied.[12,13,42] These calculations have been performed by using the geometries optimized for this theory level and using TMS as reference.

Result and Discussion

Structural analysis

Geometry optimization

Two different stable conformations were obtained from the potential energies curves for all used methods. The energy difference among them at B3PW91 and B3P86 calculation level are respectively, 1.9 kJ/mol and 1.6 kJ/mol, whereas by using the B3LYP method it is 1.80 kJ/mol. These values are fairly next to those theoretically reported values by Vazquez *et al.*[43] for this compound with the MP2 method (1.3 kJ/mol). These lower values probably indicate the flexibility of the molecular system for the rotation around the O13-C6-N1-C2 dihedral angle. Both conformations obtained from calculated potential energy curve, of C_1 symmetry, according to the syn- and anti-position of the oxygen atom with respect to the N3 atom, are named *syn* and *anti* conformers, respectively, as shown in Fig. 1. The total and relative energies of the two stable conformations of **1** at B3LYP level using 6–31 G* and 6-311++G** basis sets are given in Table 1. In all cases, the calculations in the gas phase, predict that the energy of the *anti* conformer is slightly lower than the one corresponding to *syn* conformer. Nevertheless, due to the smaller energy difference between them, both conformers are expected to be in the liquid phase. A comparison between the calculated geometrical parameters for the N-(2′-furyl)-imidazole and the corresponding experimental values of 2-(2′-furyl)-1*H*-imidazole compound are presented in Table S2 (Supporting Information). Note that the calculated parameters for the two conformers are practically independent on the basis set employed. On the other hand, the predicted bond lengths for this compound are always longer than the corresponding experimental one of 2-(2′-furyl)-1*H*-imidazole compound. Those results only show differences for the C4-C5-N1 and C6-C10-C11 bond angles. These slightly differences between the two compounds could be attributed to the fact that, in the 2-(2′-furyl)-1*H*-imidazole, the two rings are coplanar between them, thus favoring resonance effects, while in **1** both rings are not coplanar.

The stability of the *anti* conformer in relation to the *syn* conformer was investigated by using electrostatic potential maps.[22,23] The molecular electrostatic potential values for two conformers by using 6-31G* and 6-311++G** basis sets are given in Table S3 (Supporting Information), while Fig. 2 shows the electrostatic potential maps for *anti* and *syn* conformers. The atomic charges derived from the ESPs and natural atomic charges were also analyzed by using the 6-311++G** basis set and the corresponding values are given in Table S4 (Supporting Information). The important factor responsible for the lesser stability of the *syn* conformer is the electrostatic repulsion between the two positive charges on H9 and H14 atoms and between the two lone pairs on N3 and O13 atoms. Hence, a strong red colour on both atoms (from $-9.347.10^{-2}$ to $9.347.10^{-2}$ a.u. for the *anti* conformer and from $-9.313.10^{-2}$ to $9.313.10^{-2}$ a.u. for the *syn* conformer) is observed in Fig. 2. Moreover, the possible stabilizing electrostatic interaction between the H9 and O13 atoms in the *anti* conformer is slightly higher than the corresponding to the H7 and O13 atoms of the *syn* conformer. However, due to the little difference in the electrostatic potential maps and in energy values, both conformers can be expected to be in the liquid state.

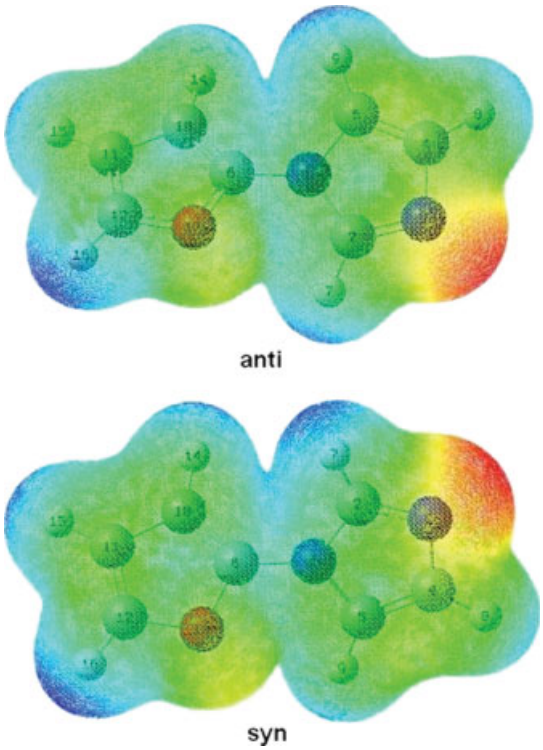

Figure 2. Calculated electrostatic potential surfaces on the molecular surfaces of *anti* and *syn* conformers of N-(2′-furyl)-imidazole. B3LYP functional and 6-31G* basis set. Isodensity value of 0.005. For color ranges see text.

NBO and AIM analyses

The stability of the two conformers of **1** was also investigated by NBO[20,28] and AIM[21] calculations. The second-order perturbation energies $E^{(2)}$ (donor → acceptor) that involve the most important delocalization are given in Table 2. The $E^{(2)}$ term referring to the second-order perturbational energy stabilization, $E^{(2)} = q_i[F(i,j)^2/(\varepsilon j - \varepsilon i)]$, where $F(i,j)$ is the Fock matrix element between an occupied orbital i and an unoccupied orbital j. $F(i,j)$ is proportional to the overlap between orbitals i and j. $\varepsilon(j) - \varepsilon(i)$ is the energy difference between orbitals i and j, and q_i is the occupancy of donor orbital i. After an analysis of the results, we found that the contribution of the $\Delta E_{\sigma-\sigma^*}{}^{(2)}$ and $\Delta E_{\pi-\pi^*}{}^{(2)}$ is practically the same for both conformers. The stabilizations energies for the LP(1)N1 → π^* C2-N3 and LP(1)N1 → π^* C4-C5 charge-transfers are slightly larger for *anti* conformer than *syn* conformer. The main electronic densities (ρ) calculated from to topological property

Table 1. Calculated total energy (E) and relative energy (ΔE) and dipolar moments (in Debyes) for the two conformers of N-(2′-furyl)-imidazole

Conformer	E (B3LYP/6-31G*) (Hartrees)	ΔE kJ/mol	μ	E (B3LYP/6-311++G**) (Hartrees)	ΔE kJ/mol	μ
syn	−455.03834901	1.8	3.80	−455.16160715	2.2	3.99
anti	−455.03903057	0	3.63	−455.16243953	0	3.82

Journal of RAMAN SPECTROSCOPY

Table 2. Main delocalization energy (in kJ/mol) for the two conformers of N-(2′-furyl)-imidazole

B3LYP/6-311++G** Method		
E(2) (donnor → aceptor)	*anti*	*syn*
σN1-C2 → σ*C6-C10	7.90	7.69
σN1-C5 → σ*C6-C10	7.27	7.32
σN1-C5 → π*C6-C10	2.55	3.14
σC6-C10 → σ*N1-C5	11.62	11.50
LP(1)N1 → π*C2-N3	171.59	168.91
LP(1)N1 → π*C4-C5	115.08	114.91
LP(1)N1 → π*C6-C10	91.29	116.83
LP(2)O → π*C6-C10	123.56	124.94
LP(2)O → π*C11-C12	103.71	101.74

analysis for two conformers are shown in Table S5 (Supporting Information). Again, there is a little difference in the topological properties between both conformers. Those results show a slightly small increase in the electronic density for the C6–O13 and N1–C2 bonds in the *syn* conformer in relation to the *anti* conformer. This effect could also be another reason for the minor stability of the *syn* conformer.

NMR results

A comparison between the experimental and calculated chemical shifts for the C and H atoms are given in Tables S6 and S7 (Supporting Information), respectively. The calculation results show that the GIAO method[41] reproduces quite well the ^{13}C and ^{1}H experimental chemical shifts values as shown by the calculated Root Mean Square Deviations (RMSD) values for each conformer. Furthermore, the shifts of the H atoms for both structures are similar in both conformers and practically equal to the average values. As expected, the latter values have a better agreement with the experimental data, provided both conformers are present in the solution.

Vibrational analysis

The previous structural analysis predicts that both conformers of **1** can be present in the liquid phase. Thus, the bands associated to the different normal modes of the two conformers should be observed in the vibrational spectra of the sample. For a complete assignment of the experimental bands of N-(2′-furyl)-imidazole, the theoretical calculations for each conformer at the B3LYP/6-311++G** level combined with Pulay's SQMFF methodology[35–37] and a comparison with related molecules[12,13,42,44–47] were considered. Both conformers have 42 normal active modes of vibration both in infrared and Raman spectra and all modes have A symmetry. The vibrational experimental spectra are shown in Fig. 3, while a comparison between the recorded infrared spectrum in the liquid phase for **1** and the corresponding calculated one are shown in Fig. 4. The populations were calculated with the B3LYP/6-311++G** energy difference by using the Boltzmann statistics, for a population relation *anti : syn* of 1 : 1 and 2 : 1 for each conformer. The resulting IR spectra are shown in Fig. 4. The calculated spectra for the two conformers and the calculated spectrum, taking into account the conformational populations (2 : 1 ratio) reproduce rather well some bands of the experimental spectrum. The assignment of the vibrational normal modes is shown in Table 3. It is observed that some modes, such as the ν_{14}, ν_{22}, ν_{37}, indicate the presence of the two conformers in the experimental IR spectrum.

Assignment of the bands: Region 4000–1000 cm^{-1}

The broad band in the 3200–3000 cm^{-1} region in the infrared and Raman spectra of the solid substance can be assigned to C–H stretching modes. Thus, the FSD procedure was carried out in this region for the purpose of identifying each band component. Only five bands localized at 3155, 3151, 3125, 3122 and 3120 cm^{-1} were obtained with the FSD procedure and they are associated with the C–H stretching modes. The remaining expected C–H stretching mode was attributed to the band in the Raman spectrum at 3101 cm^{-1}.

The most intense band at 1625 cm^{-1} in the IR spectrum is mainly assigned to the C=C stretching mode of the furane ring, which it is coupled with the ring-ring stretching mode. The two pairs of

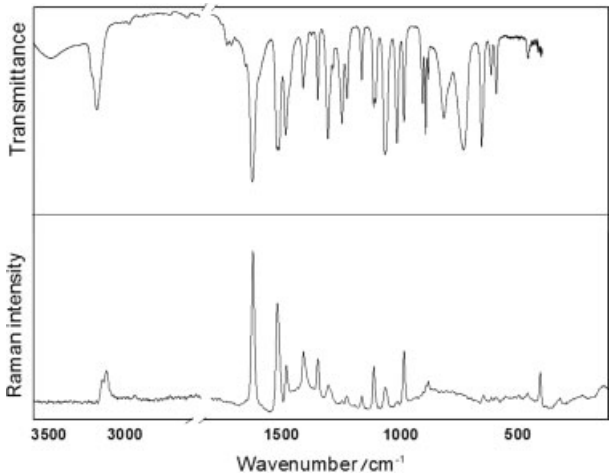

Figure 3. Infrared (upper) and Raman spectra (bottom) of the liquid substance.

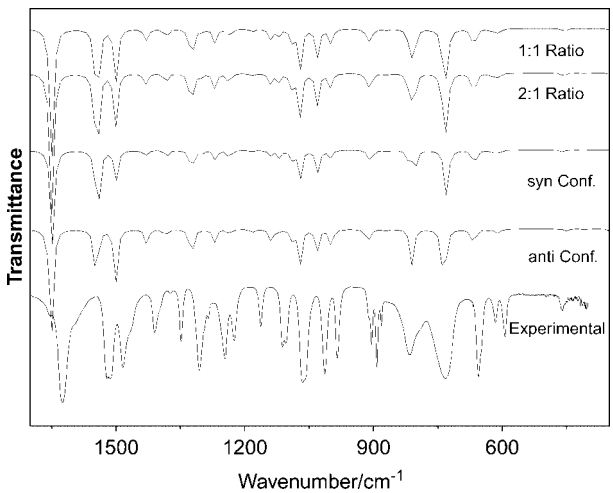

Figure 4. Comparison between the infrared experimental spectrum of N-(2′-furyl)-imidazole with the calculated infrared spectra for anti and syn conformers from B3LYP/6-311++G** frequencies and intensities using Lorentzian band shapes (for a population relation *anti: syn* of 1 : 1 and 2 : 1 for each conformer).

Table 3. Observed and calculated wavenumbers (cm^{-1}) and assignments for N-(2′-furyl)-imidazole

Mode	IR (liquid)	Raman (liquid)	Calculated *anti*[a]	Calculated *syn*[a]	Calc. SQM *anti*[b]	Calc. SQM *syn*[b]	Assignment
1	3 155 sh		3288	3290	3167	3154	ν(C–H)
2	3151 sh	3150 (9)	3282	3279	3159	3144	ν(C–H)
3	3126 s	3125 (16)	3262	3263	3137	3128	ν(C–H)
4	3122 s	–	3249	3260	3134	3126	ν(C–H)
5	3120 s	3118 sh	3247	3248	3130	3113	ν(C–H)
6	–	3101 (4)	3244	3244	3116	3110	ν(C–H)
7	1625 vs	1623 (100)	1651	1649	1599	1590	ν(C=C), $\nu(C-N)_{inter-ring}$
8	1521 s	1520 (68)	1546	1551	1486	1498	ν(C=C)
9	1511 s		1545	1542	1473	1489	ν(C=C), β(C–H)
10	1483 s	1482 (30)	1501	1501	1434	1453	ν(C=N), β(C–H)
11	1410 m	1408 (37)	1428	1433	1364	1390	β(C–H), ν(C–C)
12	1374 w	1378 sh	1385	1383	1323	1334	ν(C–C), ν(C–N)
13	1348 m	1348 (31)	1324	1325	1286	1287	β(C–H)
14	1305 s	1305 (15)		1303		1266	ν(C–N), β(C–H)
	1285 w		1295		1251		ν(C–N), β(C–H)
15	1245 s	1246 (5)	1270	1268	1234	1235	β(C–H), ν(C–N)
16	1224 m	1227 (10)	1236	1236	1191	1198	ν(C–N), ν(C=C)
17	1162 m	1162 (7)	1183	1183	1131	1145	ν(C–O), β(C–H)
18	1112 s	1113 (59)	1139	1141	1101	1100	β(C–H), ν(C=C)
19	1104 s	1089 (1)	1125	1120	1061	1087	ν(C–N)
20	1065 vs	1065 (12)	1090	1090	1026	1051	ν(C–O), ν(C–C)
21	1059 sh	–	1071	1071	1020	1037	β(C–H), ν(C–C)
22	1014 vs	1013 (4)	1031		994		ν(C–C), β(C–H)
	1012 sh			1030		1000	ν(C–C), β(C–H)
23	984 s	985 (33)	998	1001	955	978	βR_1 (i), βR_2 (i), β(C–H)
24	910 sh	–	915	916	913	908	βR_2 (i), βR_1 (i), βR_1 (f)
25	904 m	–	911	908	904	899	βR_1 (f), βR_2(i), βR_2 (f)
26	892 vs	892 sh	900	900	898	893	βR_2 (f), βR_1 (f)
27	882 w	882 (15)	880	877	890	868	γ(C–H)
28	–	–	871	866	883	857	γ(C–H)
29	816 m	–	812	816	843	806	γ(C–H)
30	793 sh	–	810	802	805	792	γ(C–H)
31	737 vs	–	736	730	758	720	γ(C–H)
32	733 vs	–	734	725	743	716	γ(C–H)
33	656 vs	–	672	668	660	649	τR_2 (f), τR_1 (f)
34	650 sh	649 (12)	665	664	646	643	τR_1 (f)
35	615 m	615 (6)	626	622	621	604	τR_2 (i), $\gamma(C-N)_{ring-ring}$, τ_{rings}
36	594 m	596 (6)		606		587	τR_1 (i), τR_2(i)
	593 m		608		586		τR_1 (i), τR_2(i)
37	462 m	463 (10)		457		451	$\beta(N-C)_{ring-ring}$
	459 sh		451		443		$\beta(N-C)_{ring-ring}$
38	–	409 (22)	406	409	392	399	$\nu(C-N)_{ring-ring}$, βR_1 (i)
39		325 (8)	346	332	352	324	$\gamma(C-N)_{ring-ring}$,
40		138 (8)	138	147	136	145	$\beta(C-N)_{ring-ring}$
41		–	106	109	111	106	τ_{rings}, $\gamma(C-N)_{ring-ring}$
42		–	49	36	35	35	Butt.
RMSD (cm^1)			7.43	7.33	2.93	2.85	

ν, stretching; β, in-plane deformation; γ, out-of-plane deformation; τ, torsion; Butt., butterfly; f, furyl; i, imidazole; R, ring, s, strong; m, medium; w, weak; v, very; sh, shoulder.
[a] B3LYP/6-311++G**.
[b] From scaled quantum mechanics force field.

overlapped bands localized at 1521 and 1511 cm^{-1} are assigned to the remaining C=C stretching modes.

In agreement with the calculation and according to the infrared spectra of similar compounds[12,13,42], the band at 1483 cm^{-1} was assigned to the N=C stretching modes for both conformers. The band in the IR spectrum at 1374 cm^{-1}, because of their PED contribution and according to related molecules[12,13] is mainly associated to the C–C stretching mode for both conformers. The

bands at 1305/1285 cm^{-1} are assigned to the C-N stretching for the *syn* and *anti*, respectively, while the two remaining modes are attributed to the bands at 1224 and 1104 cm^{-1} as shown in Table 3. In this region, six bands are also expected in the plane deformation, βC-H. Five of them are assigned to the bands at 1410, 1348, 1245, 1212 and 1059 cm^{-1}, while the remaining band appears splitted in two bands at 1014 and 1012 cm^{-1} for the *anti* and *syn* conformer, respectively. The bands localized in the infrared spectrum of the liquid phase at 1162 and 1065 cm^{-1} are related to two C-O stretching modes of the furan ring and they appear displaced toward lower wavenumbers in relation to the 2-(2′-furyl)-1*H*-imidazole.[12]

Region below 1000 cm^{-1}

In this region, the imidazole and furan ring deformation are predicted for the calculation with higher PED contribution. Hence, the bands at 984 and 910 cm^{-1} are associated to the βR_1 (i) and βR_2 (i) modes of the imidazole moiety for both conformers, while those corresponding to the furan ring, βR_1 (f) and βR_2 (f) deformation modes, for the two conformers are assigned to the bands at 904 and 892 cm^{-1}, respectively.

The two broad IR bands between 850 and 700 cm^{-1} were solved by using the FSD method that allowed to identify only five out of the six expected bands associated to the C-H out-of-plane deformation, γC-H, as shown in Table 4. In accordance with the wavenumbers reported for previously studied molecules[12,42], the bands at 656 and 650 cm^{-1} were assigned to the furan ring torsions modes, and the bands at 615 and 594/593 cm^{-1} were assigned to those corresponding to imidazole ring for both conformers.

In the lower wavenumber region, the inter-ring modes can be seen. One of the two expected inter-ring bendings, βN-C is assigned to the pair of bands at 462/459 cm^{-1} for *syn* and *anti* conformers, respectively, while the remaining mode is assigned to the band localized at 138 cm^{-1} in the Raman spectrum. The calculations predict the ring-ring stretching mode for *anti* conformer at 392 cm^{-1} and for *syn* conformer at 399 cm^{-1}; accordingly, the band observed at 409 cm^{-1} in the infrared spectrum is assigned to these modes.

Finally, the band observed in the Raman spectrum at 325 cm^{-1} was assigned to the out-of-plane inter-ring mode, $\gamma(C-N)_{ring-ring}$. Unfortunately, the butterfly mode, defined by Fogarasi *et al*.[48] for the two ring systems and the inter-ring τC–C twisting mode, could not be assigned in the experimental spectra, due to the little resolution of the Raman spectrum in the region below 120 cm^{-1}.

Force field

The scaling procedure was carried out following the method described in the computational detail section. The RMSD obtained by comparing the experimental and calculated wavenumbers from B3LYP/6-311++G** are 7.43 cm^{-1} for *anti* conformer and 7.33 cm^{-1} for the other conformer, which were decreased up to 2.93 and 2.85 cm^{-1} respectively by using the scale factors from Refs. [35–37]. The SQMFF was employed to calculate the internal force constants which are compared with the corresponding calculated values of the furan and imidazole compounds at B3LYP/6-311++G** level. The scaled force constants are given in Table S8 (Supporting Information). The comparison among them shows that in general the force constants of the N-(2′-furyl)-imidazole compound are in agreement with the ones previously calculated for the 2-(2′-furyl)-1*H*-imidazole compound.

Conclusions

The main conclusions of the present work are summarized below.

The N-(2′-furyl)-imidazole was prepared and characterized by infrared and Raman spectroscopic techniques in the liquid state and also by NMR in solution.

DFT calculations suggest the existence of two molecular conformations *syn* and *anti*, the *anti* conformation being the most stable in the gas phase, while the energy values would indicate that the two conformations are in different populations (probably *anti : syn* ratio 2 : 1) in this phase.

The calculated equilibrium energy and the computed bond lengths and angles for the two conformers are independent on the employed basis sets.

The differences in stability between both conformers were explained in terms of the atom partial charges determined from the most appropriate mapping of the electrostatic potential of each molecule.

The calculated harmonic vibrational wavenumbers for **1** are consistent with the observed liquid state, infrared and Raman spectra. The presence in the liquid of both conformers was detected in the IR spectrum and a complete assignment of the vibrational modes was accomplished.

- A SQM force field was obtained for *syn* and *anti* conformers of N-(2′-furyl)-imidazole after scaling the theoretically obtained force constants to minimize the difference between observed and calculated wavenumbers.

Acknowledgments

We thank Prof. Tom Sundius for authorizing the use of the MOLVIB Program. We also thank CONICET (Consejo Nacional de Investigaciones Científicas y Técnicas) and CIUNT (Consejo de Investigaciones de la Universidad Nacional de Tucumán) for their financial support.

Supporting information

Supporting information may be found in the online version of this article.

References

[1] A. Salerno, I. A. Perillo, *Molecules* **2005**, *10*, 435.
[2] B. Szabo, *Pharmacol. Ther.* **2002**, *93*, 1.
[3] J. C. Chang, P. C. Ulrich, R. Bucala, A. Cerami, *J. Biol. Chem.* **1985**, *260*(13), 7970.
[4] A. Salerno, V. Ceriani, I. A. Perillo, *J. Heterocycl. Chem.* **1992**, *29*, 1725.
[5] Tanabe Seiyaku Co. Ltd. Japan Kokai Tokyo Koho JP 60 51,176, *Chem. Abstr.* **1985**, *103*, 141 951t.
[6] C. Farsang, J. Kapocsi, *Brain Res. Bull.* **1999**, *49*(5), 317.
[7] J. F. Hussain, F. Miall, P. Patil, D. Miller, D. A. Kendall, V. G. Wilson, *Fundam. Clin. Pharmacol.* **1992**, *6*(1), P13.
[8] S. L. F. Chan, C. A. Brown, N. G. Morgan, *Eur. J. Pharmacol.* **1993**, *230*, 375.
[9] A. Kornicka, F. S1czewski, M. Gdaniec, *Molecules* **2004**, *9*, 86.
[10] F. S1czewski, J. S1czewski, M. Gdaniec, *Chem. Pharm. Bull.* **2001**, *49*(9), 1203.
[11] R. D. Enriz, E. A. Jáuregui, F. Tomas-Vert, *J. Mol. Struct. (Teochem)* **1994**, *306*, 115.
[12] A. E. Ledesma, S. A. Brandán, J. Zinczuk, O. Piro, J. J. López González, A. Ben Altabef, *J. Phys. Chem. Org.* **2008**, *21*(12), 1086.
[13] J. Zinczuk, A. E. Ledesma, S. A. Brandán, O. E. Piro, J. J. López-González, A. Ben Altabef. *Submitted*.

[14] (a) M. L. Quan, P. Y. S. Lam, Q. Han, D. J. P. Pinto, M. Y. He, R. Li, C. D. Ellis, C. G. Clark, C. A. Teleha, J. H. Sun, R. S. Alexander, S. Bai, J. M. Luettgen, R. M. Knabb, P. C. Wong, R. R. Wexler, *J. Med. Chem.* **2005**, *48*, 1729; (b) B. Dyck, V. S. Goodfellow, T. Phillips, J. Grey, M. Haddaach, M. Rowbottom, G. S. Naeve, B. Brown, J. Saunders, *Bioorg. Med. Chem. Lett.* **2004**, *14*, 1151; (c) J. M. Smallheer, R. S. Alexander, J. Wang, S. Wang, S. Nakajima, K. A. Rossi, A. Smallwood, F. Barbera, D. Burdick, J. M. Luettgen, R. M. Knabb, R. R. Wexler, P. K. Jadhav, *Bioorg. Med. Chem. Lett.* **2004**, *14*, 5263.
[15] (a) L. P. Beletskaya, A. V. Cheprakov, *Coord. Chem. Rev.* **2004**, 2337; (b) S. V. Ley, A. W. Thomas, *Angew. Chem.* **2003**, *42*, 5400; (c) K. Kunz, U. Scholz, D. Ganser *Synlett* **2003**, 2428.
[16] A. R. Altman, E. D. Koval, S. L. Buchwald, *J. Org. Chem.* **2007**, *72*, 6190.
[17] A. E. Reed, L. A. Curtis, F. Weinhold, *Chem. Rev.* **1988**, *88*(6), 899.
[18] J. P. Foster, F. Weinhold, *J. Am. Chem. Soc.* **1980**, *102*, 7211.
[19] A. E. Reed, F. Weinhold, *J. Chem. Phys.* **1985**, *83*, 1736.
[20] R. F. W. Bader, *Atoms in Molecules, A Quantum Theory*, Oxford University Press: Oxford, **1990**, ISBN: 0198558651.
[21] F. Biegler-Köning, J. Schönbohm, D. Bayles, *J. Comput. Chem.* **2001**, *22*, 545.
[22] N. Sadlej-Sosnowska, *J. Phys. Chem. A* **2007**, *111*, 11134.
[23] A. Vektariene, G. Vektaris, J. Svoboda *11th International Electronic Conference On Synthetic Organic Chemistry (ECSOC-11)*, Lugo, Spain, **2007**.
[24] D. Becke, *J. Chem. Phys. Rev.* **1993**, *98*, 5648.
[25] C. Lee, W. Yang, R. G. Parr, *Phys. Rev.* **1988**, *B37*, 785.
[26] J. P. Perdew, J. A. Chevary, S. H. Vosko, K. A. Jackson, M. R. Pederson, D. J. Singh, C. Fiolhais, *Phys. Rev.* **1993**, *B 48*, 4978.
[27] J. P. Perdew, *Phys. Rev.* **1986**, *B 33*, 8822.
[28] E. D. Gledening, J. K. Badenhoop, A. D. Reed, J. E. Carpenter, F. Weinhold, *NBO 3.1; Theoretical Chemistry Institute*, University of Wisconsin: Madison, **1996**.
[29] B. H. Besler, K. M. Merz Jr, P. A. Kollman, *J. Comp. Chem.* **1990**, *11*, 431.
[30] M. J. Frisch, G. W. Trucks, H. B. Schlegel, G. E. Scuseria, M. A. Robb, J. R. Cheeseman, J. A. Montgomery Jr., T. Vreven, K. N. Kudin, J. C. Burant, J. M. Millam, S. S. Iyengar, J. Tomasi, V. Barone, B. Mennucci, M. Cossi, G. Scalmani, N. Rega, G. A. Petersson, H. Nakatsuji, M. Hada, M. Ehara, K. Toyota, R. Fukuda, J. Hasegawa, M. Ishida, T. Nakajima, Y. Honda, O. Kitao, H. Nakai, M. Klene, X. Li, J. E. Knox, H. P. Hratchian, J. B. Cross, C. Adamo, J. Jaramillo, R. Gomperts, R. E. Stratmann, O. Yazyev, A. J. Austin, R. Cammi, C. Pomelli, J. W. Ochterski, P. Y. Ayala, K. Morokuma, G. A. Voth, P. Salvador, J. J. Dannenberg, V. G. Zakrzewski, S. Dapprich, A. D. Daniels, M. C. Strain, O. Farkas, D. K. Malick, A. D. Rabuck, K. Raghavachari, J. B. Foresman, J. V. Ortiz, Q. Cui, A. G. Baboul, S. Clifford, J. Cioslowski, B. B. Stefanov, G. Liu, A. Liashenko, P. Piskorz, I. Komaromi, R. L. Martin, D. J. Fox, T. Keith, M. A. Al-Laham, C. Y. Peng, A. Nanayakkara, M. Challacombe, P. M. W. Gill, B. Johnson, W. Chen, M. W. Wong, C. Gonzalez, J. A. Pople, *Gaussian 03, Revision B.01*, Gaussian, Inc.: Pittsburgh, **2003**.
[31] T. Sundius, *J. Mol. Struct.* **1990**, *218*, 321.
[32] T. Sundius, *Vib. Spectrosc.* **2002**, *29*, 89.
[33] P. Pulay, G. Fogarasi, G. Pongor, J. E. Boggs, A. Vargha, *J. Am. Chem. Soc.* **1983**, *105*, 7037.
[34] A. B. Nielsen, A. J. Holder, *Gauss View 3.0, User's Reference*, Gaussian Inc.: Pittsburgh, **2000–2003**.
[35] G. Rauhut, P. Pulay, *J. Phys. Chem.* **1995**, *99*, 3093.
[36] G. Rauhut, P. Pulay, *J. Phys. Chem.* **1995**, *99*, 14572.
[37] F. Kalincsák, G. Pongor, *Spectrochim. Acta A* **2002**, *58*, 999.
[38] J. K. Kauppinen, D. J. Moffatt, H. H. Mantsch, D. G. Cameron, *Appl. Spectrosc.* **1981**, *35*, 271.
[39] J. K. Kauppinen, D. J. Moffatt, D. G. Cameron, H. H. Mantsch, *Appl. Opt.* **1981**, *20*, 1866.
[40] J. K. Kauppinen, D. J. Moffatt, M. R. Holberg, H. H. Mantsch, *Appl. Spectrosc.* **1991**, *45*, 411.
[41] R. Ditchfield, *Mol. Phys.* **1974**, *8*, 397.
[42] A. E. Ledesma, J. Zinczuk, A. Ben Altabef, J. J. López-González, S. A. Brandán. *Submitted*.
[43] J. Vázquez, J. J. López González, L. Ballester, J. Boggs, *J. Mol. Struc.* **1997**, *393*, 97.
[44] F. Billes, H. Böhling, M. Ackermann, M. Kudra, *J. Mol. Struct.* **2004**, *672*, 1.
[45] S. T. King, *J. Phys. Chem.* **1970**, *74*, 2133.
[46] T. D. Klots, R. D. Chirrido, W. V. Stele, *Spectrochim. Acta A* **1994**, *50*, 765.
[47] A. El-Azhary, R. H. Hilal, *Spectrochim. Acta A* **1997**, *53*, 1365.
[48] G. Fogarasi, X. Zhou, P. W. Taylor, P. Pulay, *J. Am. Chem. Soc.* **1992**, *105*, 7037.